



ELSEVIER

Contents lists available at ScienceDirect

## Thin Solid Films

journal homepage: [www.elsevier.com/locate/tsf](http://www.elsevier.com/locate/tsf)

# Role of deposition temperature on the mechanical and tribological properties of Cu and Cr co-doped diamond-like carbon films



Lili Sun<sup>a</sup>, Xiao Zuo<sup>a</sup>, Peng Guo<sup>a</sup>, Xiaowei Li<sup>b</sup>, Peiling Ke<sup>a,c</sup>, Aiyang Wang<sup>a,c,\*</sup>

<sup>a</sup> Key Laboratory of Marine Materials and Related Technologies, Zhejiang Key Laboratory of Marine Materials and Protective Technologies, Ningbo Institute of Materials Technology and Engineering, Chinese Academy of Sciences, Ningbo 315201, PR China

<sup>b</sup> Computational Science Center, Korea Institute of Science and Technology, Seoul 136-791, Republic of Korea

<sup>c</sup> Center of Materials Science and Optoelectronics Engineering, University of Chinese Academy of Sciences, Beijing 100049, PR China

## ARTICLE INFO

## Keywords:

Copper  
Chromium  
Diamond-like carbon  
Mechanical property  
Tribological behavior  
Direct-current magnetron sputtering  
Anode-layer ion beam source

## ABSTRACT

In this study, Cu and Cr co-doped diamond-like carbon (Cu/Cr-DLC) films were synthesized using a hybrid ion beam deposition system. The effects of deposition temperature on the metal content, hardness and wear behavior of Cu/Cr-DLC films were investigated. Particularly, an optical emission spectroscopy was applied to characterize the plasma at different deposition temperatures. Results showed that the intensities of Cu and Cr spectral lines decreased dramatically as the temperature increased from 60 to 250 °C. The concentrations of Cu and Cr decreased from 18.1 to 2.7 at.% and 10.5 to 2.2 at.%, respectively. Meanwhile, high temperature promoted the formation of the Cr carbide phase, which was beneficial to achieve high hardness of the film. Although the residual stress increased with the rise of deposition temperature, the Cu/Cr-DLC film showed a better adhesive strength in comparison with pure amorphous carbon film. The wear resistance was also significantly improved at high deposition temperature, and only faint wear was observed when the temperature was above 150 °C. The excellent tribological performance of Cu/Cr-DLC film was mainly attributed to good mechanical properties and the formation of continuously compacted graphitized transfer film under dry sliding conditions.

## 1. Introduction

Metal-doping is of extreme importance in the scientific and engineering fields of diamond-like carbon (DLC) films owing to the contribution of lowering high intrinsic residual stress and enhancing adhesion of pure DLC films on substrate [1–3]. Meanwhile, it is also utilized to tailor the mechanical, tribological and optical properties of pure DLC films [4–6]. According to bonding characteristics, metal dopants are classified into two main categories: carbide forming elements and non-carbide forming elements. And it is worthy of note that the structures and properties of metal doped DLC (Me-DLC) films significantly depend upon the features of doped metal. By comparison, introducing the carbide forming elements, like Ti [7], Cr [8] and W [9], into DLC films could mainly improve the hardness and wear rate by the formation of hard carbide phase in the carbon matrix, but the problems of high compressive stress and brittleness still remain. Non-carbide forming elements (like Ag [10], Cu [11], Al [12]) incorporated into DLC tend to form ductile metal phases in the carbon matrix, which favors the tribological properties by increasing the toughness of the films, but both

the residual stress and hardness of film reduced drastically. Therefore, it still remains a big challenge for preparing Me-DLC films with both outstanding mechanical and tribological properties via mono metal-doping.

Recently, many researchers attempted to improve the integrated performances of DLC films by various duplex metal-doping methods. Li et al. [13] found that the introduction of low Ti/W content could effectively lower the residual compressive stress, and improve the film hardness as well as wear resistance. The duplex W-doped nanocomposite carbon-based films (such as nc-WC/a-C (Al)) also possessed a good balance among hardness, toughness, low internal stress, superior low-friction and anti-wear properties [14]. Moreover, through ab initio calculations we found that Ti/Al or Cu/Cr co-doping with appropriate metal contents could remarkably reduce the intrinsic stress of DLC films without deteriorating the mechanical properties [15,16]. And the good performance was attributed to the synergistic effects of soft ductile non-carbide forming metals and hard carbide forming ones. These bring forward a different concept to endow DLC films with superior comprehensive properties by the synergistic effect from the carbide and

\* Corresponding author at: Key Laboratory of Marine Materials and Related Technologies, Zhejiang Key Laboratory of Marine Materials and Protective Technologies, Ningbo Institute of Materials Technology and Engineering, Chinese Academy of Sciences, Ningbo 315201, PR China.

E-mail address: [aywang@nimte.ac.cn](mailto:aywang@nimte.ac.cn) (A. Wang).

<https://doi.org/10.1016/j.tsf.2019.03.034>

Received 29 August 2018; Received in revised form 18 March 2019; Accepted 28 March 2019

Available online 30 March 2019

0040-6090/ © 2019 Elsevier B.V. All rights reserved.

non-carbide forming metals. Nevertheless, an in-depth understanding of the co-doped DLC films on the relationship between the structure and properties is still required. In particular, most of previous works focused on the dependence of structural properties on co-doped metal content, sputtering current and bias voltage [14,17], the effect of substrate temperature on metal co-doped DLC films is not given enough attention. In fact, deposition temperature is an important parameter affecting the properties of DLC films. On the one hand, high temperature can increase the mobility of the particles and promote the formation of the carbide phase [18], which could maintain high hardness. On the other hand, it can promote the formation of the structural ordering of DLC films by increasing the temperature, thereby improving the tribological properties of the film [19].

Our previous study has fabricated the Cu/Cr co-doped DLC films by a hybrid ion beam deposition system [20], which obtained lower residual stress and higher hardness by accurately controlling Cu and Cr concentration. Unfortunately, the good tribological properties of DLC films were significantly destroyed. Therefore, in order to obtain high hardness and good friction performance, Cu/Cr co-doped DLC films were deposited at higher temperature in this study, the effects of the deposition temperature on the microstructure, adhesion, mechanical and tribological properties of the Cu/Cr co-doped DLC films were investigated.

## 2. Material and methods

### 2.1. Experiment

The Cu/Cr co-doped DLC films were deposited by a hybrid plasma process combining the DC magnetron sputtering (DCMS) and an anode-layer ion beam source (ALIS) [21]. P-(100) silicon wafers with thickness of  $450 \pm 20 \mu\text{m}$  were used as substrates for microstructure and properties analysis, and a thin single crystal Si with thickness of  $240 \pm 5 \mu\text{m}$  was used to estimate the residual stress. Meanwhile, a high speed steel (HSS) substrate was used to evaluate the adhesion of the Cu/Cr-DLC film deposited at  $200^\circ\text{C}$ . Acetylene precursor was supplied to the ALIS source for DLC films deposition. A composite  $\text{Cu}_{50}\text{Cr}_{50}$  (99.95% in purity) target with  $400 \text{ mm} \times 10 \text{ mm} \times 7 \text{ mm}$  in size was fixed on the DCMS source for Cu/Cr co-doping. Prior to deposition, silicon wafers were ultrasonically cleaned with acetone and alcohol for 10 min, respectively, and dried in air blow before putting into the vacuum chamber. The distance from the center of samples to ALIS and  $\text{Cu}_{50}\text{Cr}_{50}$  target was controlled at around 20 cm. The chamber was evacuated to a base pressure about  $2.7 \times 10^{-3} \text{ Pa}$ . A 10 min Ar plasma etching was performed to remove contamination layer and undesirable oxide prior to film deposition. During deposition, the films were deposited for 15 min in the mixture precursors with 65 sccm Ar gas and 15 sccm  $\text{C}_2\text{H}_2$  gas, the working pressure was about 0.39 Pa. The DC power applied to the  $\text{Cu}_{50}\text{Cr}_{50}$  target was maintained at about 1.3 kW, and the working current and voltage of the ALIS were 0.2 A and 1300  $\pm$  50 V, respectively. The deposition temperature was varied at 60, 100, 150, 200 and  $250^\circ\text{C}$  by using resistance-wire heating. The chamber temperature was measured by a K type thermocouple, which was located at the middle of the chamber. In order to achieve stable temperature, we extended the holding time until the temperature became stable. Meanwhile, a negative pulsed bias voltage of  $-100 \text{ V}$  (350 kHz, 1.1  $\mu\text{s}$ ) was applied to the substrate during both the etching and deposition processes. The deposition times of all the film were 15 min. For adhesion comparison, the pure DLC film was also deposited on HSS substrate, and the thickness of DLC film was the same as that of Cu/Cr-DLC film deposited at  $200^\circ\text{C}$ .

### 2.2. Film characterization

In order to clarify the variations in the chemical composition of the films with deposition temperature, the plasma near substrate region

was investigated through optical emission spectroscopy (OES). The emitted light from the plasma was collected by using an optical fiber connected to an Acton SpectraPro SP-2500 spectrometer (Princeton Instruments) equipped with a SpectraHub detector. The spectrometer was calibrated by typical mercury pen lamps.

The chemical bonds of deposited films were investigated by X-ray photoelectron spectroscopy (XPS, Axis Ultra-DLD, Japan) with Al (mono)  $K\alpha$  radiation. Before commencing the measurement,  $\text{Ar}^+$  ion beam was used to etch the sample surface for 3 min to remove contaminants and oxide. The cross-sectional microstructures and Cu/Cr concentration of as-deposited films were investigated by field-emission scanning electron microscopy (FESEM, S-4800, Japan) with an energy dispersive X-ray spectroscopy (EDS, Hitachi S-4800). Raman spectroscopy with a laser wavelength of 532 nm (inVia-reflex, UK) was employed to characterize the carbon atomic bond details of as-deposited films.

Hardness and Young's modulus were characterized by a load-controlled MTS NANO200 nano-indentation equipped with a Berkovich diamond tip. In order to get the sufficient resolution of a range of penetration depths, a continuous stiffness measurement (CSM) mode with a maximum indentation depth of 200 nm was selected to obtain load independent mechanical properties. Six replicate indentations were made for each sample, and took the hardness value around 10% of the thickness as the hardness of film. The residual stress was calculated according to the Stoney equation and the film/substrate curvature was determined by a stress tester (JLCST022, J&L Tech) using a laser reflection method. Scratch testing was used to evaluate the adhesion ability of the films. The tests were performed by a CSM device using a spheroconical diamond probe with an end radius of  $200 \mu\text{m}$ . The scratch length was 3 mm and the applied load was varied from 1 N to 50 N with a loading rate of 49 N/min. After the tests the films were evaluated using optical microscopy. The tribological properties of the films were measured on a rotary ball-on-disk tribometer (JLTB-02, Korea) under dry sliding conditions at  $24^\circ\text{C}$ , 56 RH%. A steel ball (SUJ2) with a diameter of 6 mm was used as the friction counter body. All the tests were performed at a sliding speed of  $50 \text{ mm s}^{-1}$  and the applied load was 5 N. The wear tracks were investigated by a surface profiler and FESEM. The composition and structure of the wear scar and debris were analyzed with Raman spectroscopy.

## 3. Results and discussion

### 3.1. Chemical composition and microstructure

The chemical composition of the deposited Cu/Cr-DLC films characterized by EDS is presented in Fig. 1(a). With the increase of deposition temperature, the contents of Cu and Cr in the films varied from 18.1 to 2.7 at.% and 10.5 to 2.2 at.%, respectively. The concentration of Cu was much higher than that of Cr in the films, which deviated from the ratio of Cu/Cr in the target. This phenomenon could be attributed to the different sputtering yields of Cu and Cr atoms [22].

Fig. 1(b) displays the changes in the emission intensities of Cu/Cr and Ar as function of the deposition temperature. When the deposition temperature increased from  $60^\circ\text{C}$  to  $250^\circ\text{C}$ , the intensities of Cr,  $\text{Cr}^+$  and Cu at 360 nm, 486 nm, 521 nm and 656 nm decreased sharply, while  $\text{Ar}^+$  and Ar intensities at 358 nm, 426 nm and 434 nm presented a similar trend. On one hand, when the deposition temperature increased, the collision frequency of the particles (including electrons and molecules) increased, which could lead more high-energy electrons to lose energy and degenerate into low-energy electrons, then decreased the ionization efficiency. As a consequence, the lower argon ion density reduced the bombardment efficiency of Cu/Cr target. On the other hand, the accumulation of carbon particles on the surface of metal target could also weaken the sputtered Cu and Cr atoms densities.

Fig. 2 illustrates the cross-sectional SEM images and thickness of the deposited Cu/Cr-DLC films. The film deposited at  $60^\circ\text{C}$  exhibited the

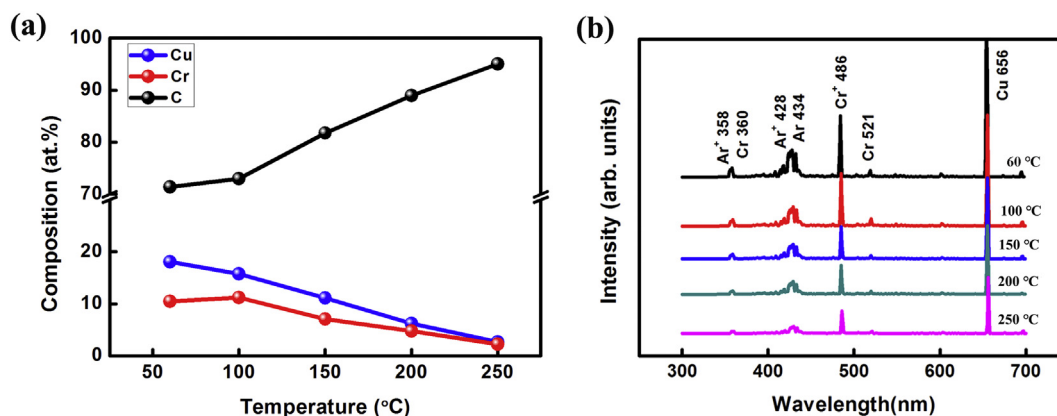


Fig. 1. (a) Compositions of the Cu/Cr-DLC films and (b) optical emission spectra of plasma as a function of the deposition temperature.

columnar microstructure which was composed of small nanoparticles. With the increase of the deposition temperature, the nanoparticles size decreased and typical amorphous feature was observed. Besides, the film thickness significantly decreased from 548 to 305 nm as the deposition temperature increased from 60 to 250 °C, which showed the same trend as the metal concentration. It meant that metal concentration dominated the deposition rate of the Me-DLC films due to a higher sputtering yield of the metal target materials [23].

In order to understand the structural evolution of films at different deposition temperatures, Raman analysis was invoked to obtain the carbon atomic bond characteristics in the Cu/Cr-DLC films. Fig. 3(a) displays the Raman spectra of the deposited films. All the spectra of the Cu/Cr-DLC films presented a broad asymmetric Raman scattering band in the range of 1000 to 1700  $\text{cm}^{-1}$ , which implied the typical structural feature of DLC films [24]. Moreover, the DLC Raman spectra could be fitted by two Gaussian peaks: D peak around 1380  $\text{cm}^{-1}$  and G peak around 1550  $\text{cm}^{-1}$  (the fitting result of film deposited at 250 °C in Fig. 3(a)) [24]. Usually, the intensity ratio of D peak to G peak ( $I_D/I_G$ ), the G peak position, and the full width at half maximum of the G peak ( $G_{FWHM}$ ) are used to monitor carbon bonding. It is known that high  $\text{sp}^2/\text{sp}^3$  ratio can make the G peak position shift to higher value of Raman

shift, while higher bond length and bond angle disorder can lead to a higher value of  $G_{FWHM}$  [25]. As shown in Fig. 3(b), the G peak position shifted from 1546  $\text{cm}^{-1}$  to 1549  $\text{cm}^{-1}$ , and slightly decreased to 1548  $\text{cm}^{-1}$  at 150 °C, then increased to 1556  $\text{cm}^{-1}$ , while the  $I_D/I_G$  first increased from 1.52 to 1.87 and then decreased to 1.62 with the deposition temperature varied from 60 to 250 °C. By contrast, the  $I_D/I_G$  ratios of the films beyond of 100 °C were higher than that of the film at 60 °C. The results indicated that the films tended to be graphitizing at high deposition temperature, which could attribute to the excess energy provided by high deposition temperature to prevent the formation of a high  $\text{sp}^3$  fraction [26]. The value of  $G_{FWHM}$  slightly increased with the rising deposition temperature, which demonstrated that the structural disorder of the films increased with the deposition temperature.

Fig. 4 presents the elemental bonding states in Cu/Cr-DLC films analyzed by XPS. In Fig. 4(a), the intensity of the Cu 2p peak decreased with the increase of deposition temperature. Except for 250 °C, the main peaks of Cu 2p<sub>3/2</sub> in all films presented the narrow symmetric shape centered at  $\sim 932$  eV, corresponding to metallic state Cu or oxide state Cu<sub>2</sub>O [19]. Unfortunately, Cu phase was difficult to be distinguished from Cu<sub>2</sub>O phase because their binding energies are too close. Generally, there is no Cu carbide forming on account of the weak bond

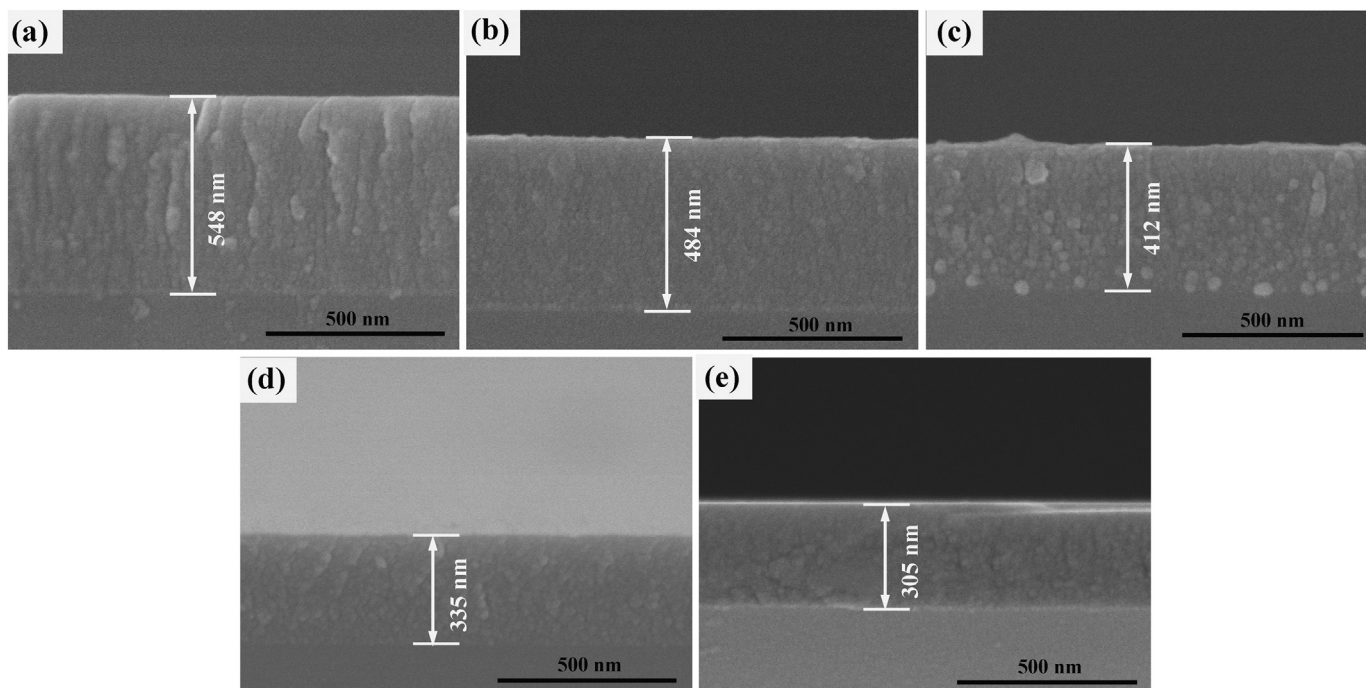


Fig. 2. The cross-sectional SEM images of the Cu/Cr-DLC films deposited at different temperatures. (a) 60 °C, (b) 100 °C, (c) 150 °C, (d) 200 °C, (e) 250 °C.

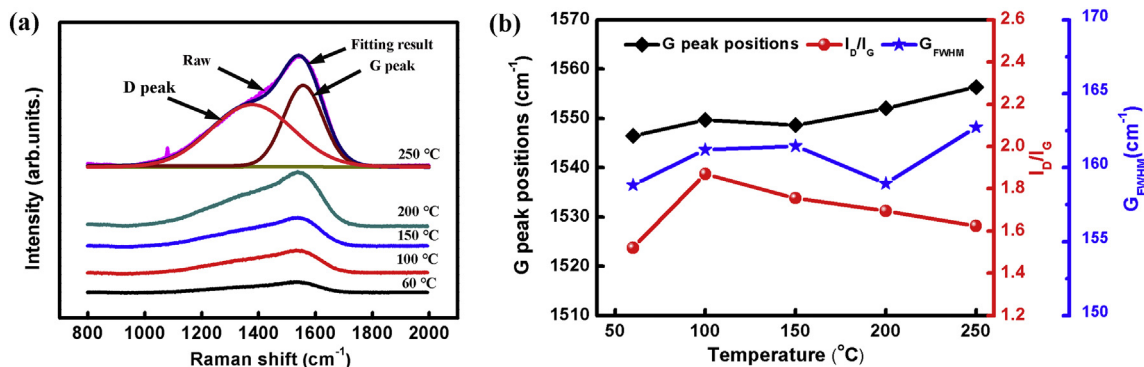


Fig. 3. (a) Raman spectra and (b) the G position,  $I_D/I_G$  and  $G_{FWHM}$  of the Cu/Cr-DLC films as a function of the deposition temperature.

between Cu and C atoms [27]. Fig. 4(b) is the normalized core level C 1s spectra of Cu/Cr-DLC films deposited at various temperatures. The C1s spectra showed large asymmetric peaks, suggesting the existence of carbon atoms in various bonding states. In particular, a binding energy around 283 eV was visible at the temperature below 250 °C, which indicated the existence of the chromium carbide. Fig. 4(c) shows typical fitting profiles of C 1s peaks for the film deposited at 200 °C. The four peaks corresponded to the  $sp^2$ -C bond around 284 eV, the  $sp^3$ -C bond around 285 eV, the C–O bond around 286 eV and the Cr–C bond around 283 eV, respectively. Moreover, the bond fractions of the C–C/C–H, Cr–C and C–O bonds in films were determined by the relative peak areas of the decomposition peaks of the C 1s spectra, and were displayed in Fig. 4(d). Interestingly, the fraction of Cr–C bond showed a sharp increase from 1.7 to 7.0% as Cr concentration decreased from 18.1 to 15.8 at.%. Even the Cr content decreased to 6.2 at.% at 200 °C, the fraction of Cr–C bond was 4.18%, which was higher than that of

film deposited at 60 °C. This result proposed that the deposition temperature was beneficial to the formation of Cr–C phase. The reason was that the thermal energy provided by high deposition temperature was enough to promote the bonding between Cr and C atoms [18]. Besides, the fraction of C–O bond in the films remained fairly constant with a value of 3.0 at.%. The presence of oxygen was caused by the insufficient vacuum during the plasma deposition process.

### 3.2. Mechanical properties and adhesion tests

Fig. 5 shows the mechanical properties on hardness, elastic modulus and H/E ratio of Cu/Cr-DLC films as a function of deposition temperature. When the deposition temperature increased from 60 °C to 100 °C, the hardness decreased slightly from  $12.2 \pm 0.17$  GPa to  $10.5 \pm 0.13$  GPa. However, the hardness and elastic modulus increased as the deposition temperature was higher than 100 °C. In

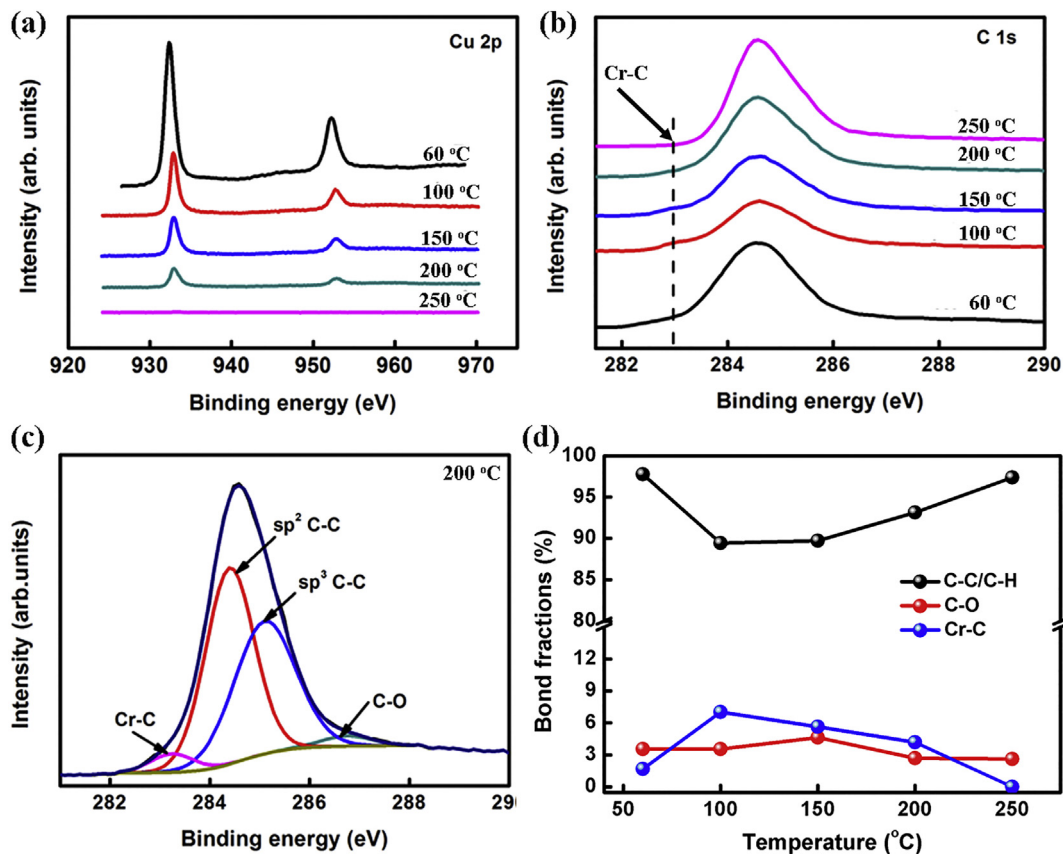


Fig. 4. (a) Cu 2p core level spectra of Cu/Cr-DLC films at various deposition temperatures; (b) High resolution XPS for C 1s; (c) Deconvolution of C 1s spectra of Cu/Cr-DLC film at 200 °C; (d) The bonding fractions of the Cr–C, C–C/C–H and C–O bonds in Cu/Cr-DLC films.

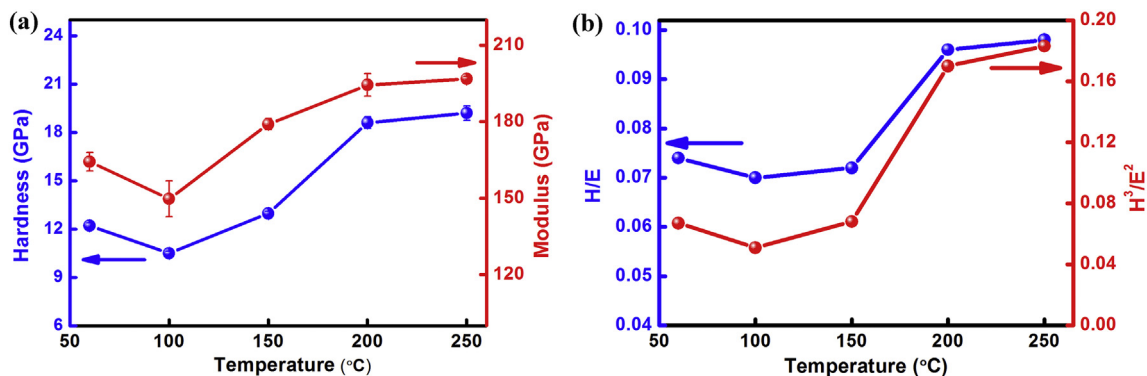


Fig. 5. (a) Hardness and elastic modulus and (b) H/E and  $H^3/E^2$  of the films as a function of deposition temperature.

special, at 250 °C, the hardness of film increased to  $19.2 \pm 0.45$  GPa, which showed similar mechanical property as the pure amorphous carbon. Combining with the Raman and XPS analysis, it could be deduced that the variation in hardness was dominated by the competition between the formation of hard nanoparticles and graphitization. First, the  $sp^2/sp^3$  ratio strongly affected the hardness of films, and higher  $sp^2$  content could be obtained at higher deposition temperature. Second, the hard Cr carbide could be easily formed with deposition temperature increased, but the formation of carbide could break the continuity of the carbon network, which could destroy the high hardness of DLC film. At low deposition temperature, a large amount of Cr carbide broken the continuity of the carbon network, and the formation of soft Cu cluster and graphitization led to the hardness to decrease. On one hand, the concentration of the Cu/Cr decreased with the increase of deposition temperature, and lower content of hard Cr carbides and soft Cu cluster could reduce the damage to the hardness of DLC films. On the other hand, high deposition temperature could increase the density of the amorphous carbon films [28], which was beneficial to improve the hardness property. With these two combined effects, the hardness of the film increased at high deposition temperature. The H/E and  $H^3/E^2$  ratios, which were indicators for the toughness of a film [29], were fairly similar to that of the hardness. The ratios slightly decreased with deposition temperature up to 100 °C, followed by a steady increase with a further increase in deposition temperature. The highest H/E (0.10) and  $H^3/E^2$  (0.18 GPa) ratios were obtained at 250 °C. The results indicated that Cu/Cr co-doping could enhance the toughness of DLC film without sacrificing hardness at appropriate deposition temperature.

Fig. 6 reveals the variation of residual stress of the films as a function of the deposition temperature. When deposition temperature increased from 60 to 150 °C, the stress increased from  $0.89 \pm 0.13$  GPa to  $2.23 \pm 0.11$  GPa. Then it slightly decreased to  $2.16 \pm 0.01$  GPa at

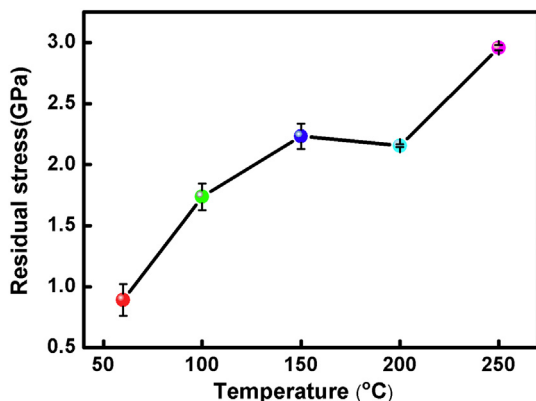


Fig. 6. Residual stress curve of Cu/Cr-DLC films deposited at different deposition temperatures.

200 °C, and significantly increased to a maximum value of  $2.70 \pm 0.02$  GPa at 250 °C. It was mainly attributed to the concentrations and existence of doped metals [20]. When the deposition temperature were 100 and 150 °C, high fraction of Cr–C bond led to high residual stress, which was because the Cr–C bond length was longer than the C–C bond length. Then the deposition temperature increased to 200 °C, proper concentrations of Cu and Cr doping were favorable to reduce the value of residual stress. However, when the deposition temperature was 250 °C, lower concentration of Cu/Cr had no significant effect on the relaxation of the distortion of C–C bond structure, resulting in an increase in the residual stress.

Fig. 7 shows the comparison of adhesion behaviors of Cu/Cr-DLC and DLC films deposited on HSS substrates. For Cu/Cr-DLC film deposited at 200 °C, the peripheral cracking was observed from the optical micrographs which might result from the different plastic deformation between film and HSS substrate. However, the micrograph of the film under the scratch track was still complete, meant the film had a high cohesion force due to its low residual stress. Through the analysis of acoustic emission signals analysis, the critical load of the Cu/Cr-DLC film was 30.5 N. On the contrary, Pure DLC film presented obvious adhesion failure before the diamond stylus penetrated the substrate at load 50 N, and the critical load was 18.7 N. It was revealed that Cu/Cr doping was beneficial to the improvement of the adhesion between DLC and HSS substrate.

### 3.3. Tribological properties

A load of 5 N was applied to detect the tribological properties of the films in ambient air, as demonstrated in Fig. 8. At low deposition temperature ( $< 150$  °C), the films presented high and fluctuating friction coefficients (Fig. 8(a)). In particular, the steady-state friction coefficient of film deposited at 60 °C showed the highest value about 0.36. The corresponding cross-section profiles of the wear track shown in Fig. 8(b) revealed a large wear depth ( $> 560$  nm), illustrating that the film had already been worn out. As the deposition temperature increased, the wear tracks of the films became smaller and shallower, which was shown in Fig. 8(c)–(d). Specially, the films deposited at 200 °C and 250 °C presented a relatively steady and low coefficient of friction  $< 0.11$ . Meanwhile, good wear resistance was obtained, and the wear track was difficult to be seen from the surface profile.

Fig. 9 presents the corresponding morphologies of the wear tracks on the films. The deepest and broadest wear track with mass of wear debris and obvious furrows was observed at 60 °C. Some small fragments of the films were even delaminated during the test. The wear tracks of the films deposited at higher temperatures became smaller and shallower. As the deposition temperature increased to 200 °C and 250 °C, there was no evidence of scratches or wear debris in the vicinity of the wear tracks.

Fig. 10 shows the SEM images and corresponding elemental

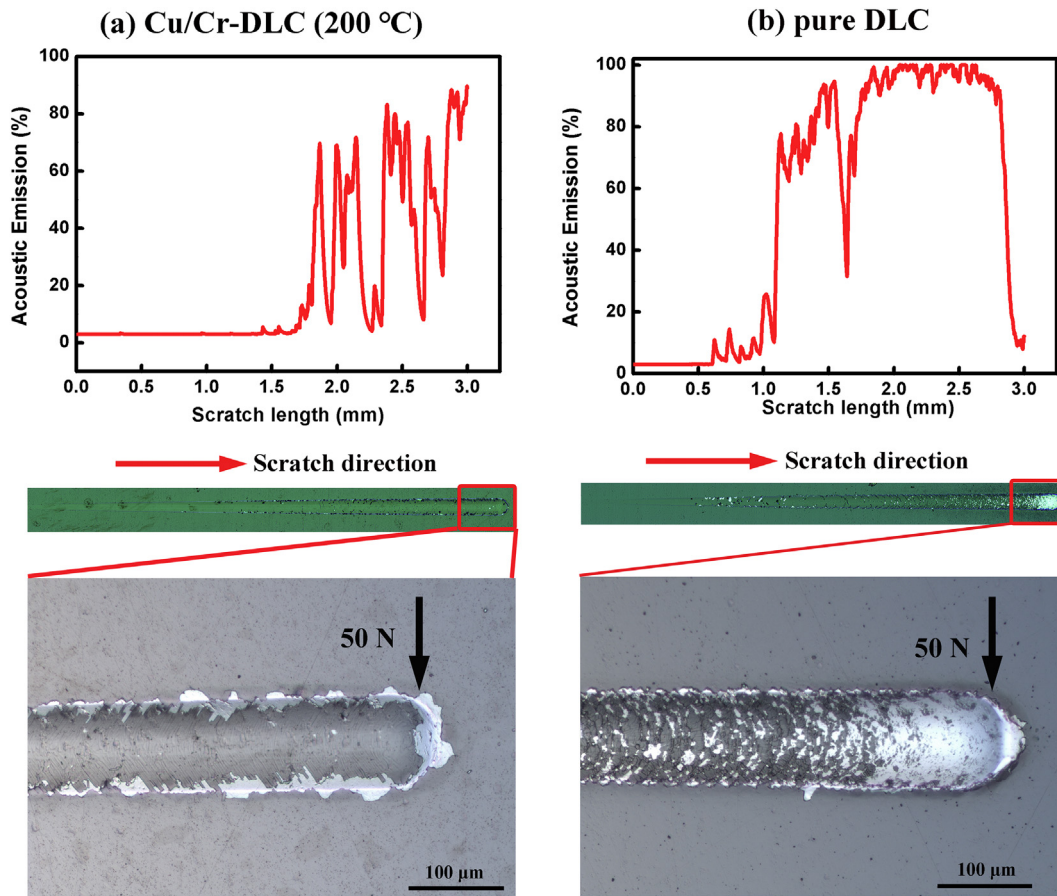


Fig. 7. Comparison of scratch test of (a) Cu/Cr-DLC (200 °C) (left) and (b) pure DLC films (right) deposited on HSS substrates. Acoustic emission curves and optical micrographs of the scratch tracks showed the failure behavior for these two films. The normal load was increased from 0 to 50 N.

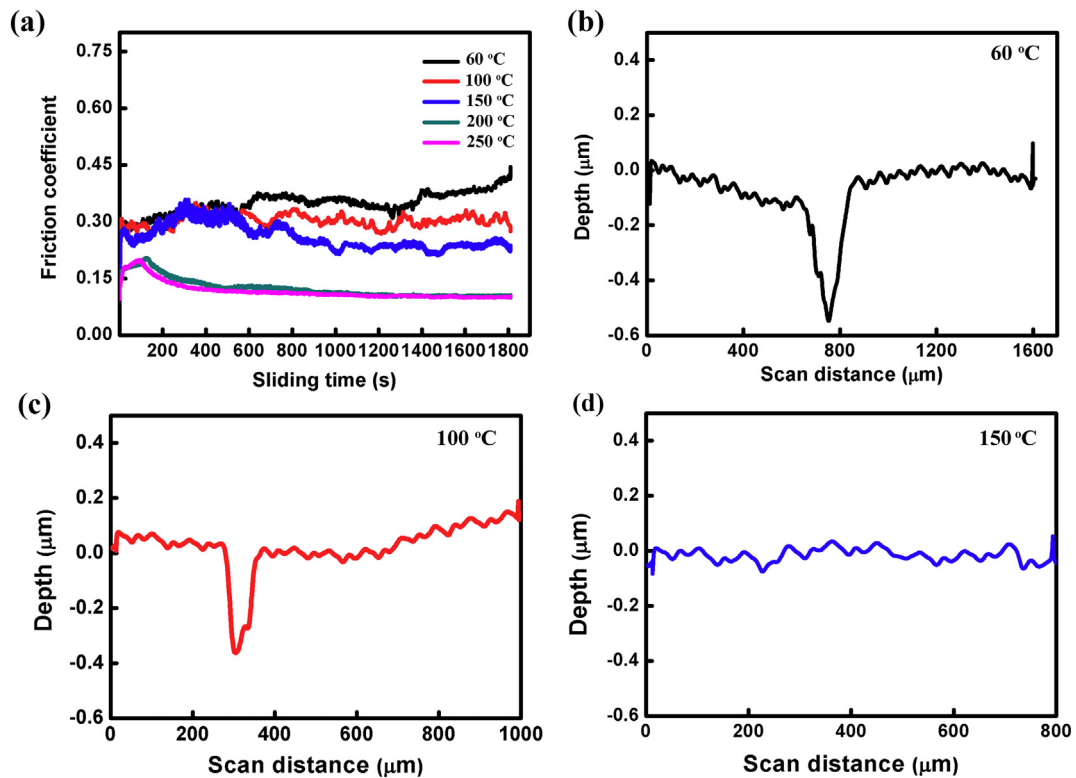


Fig. 8. (a) Friction coefficient and (b)~(d) corresponding cross-section profiles of the wear tracks for different Cu/Cr-DLC films as a function of sliding time.

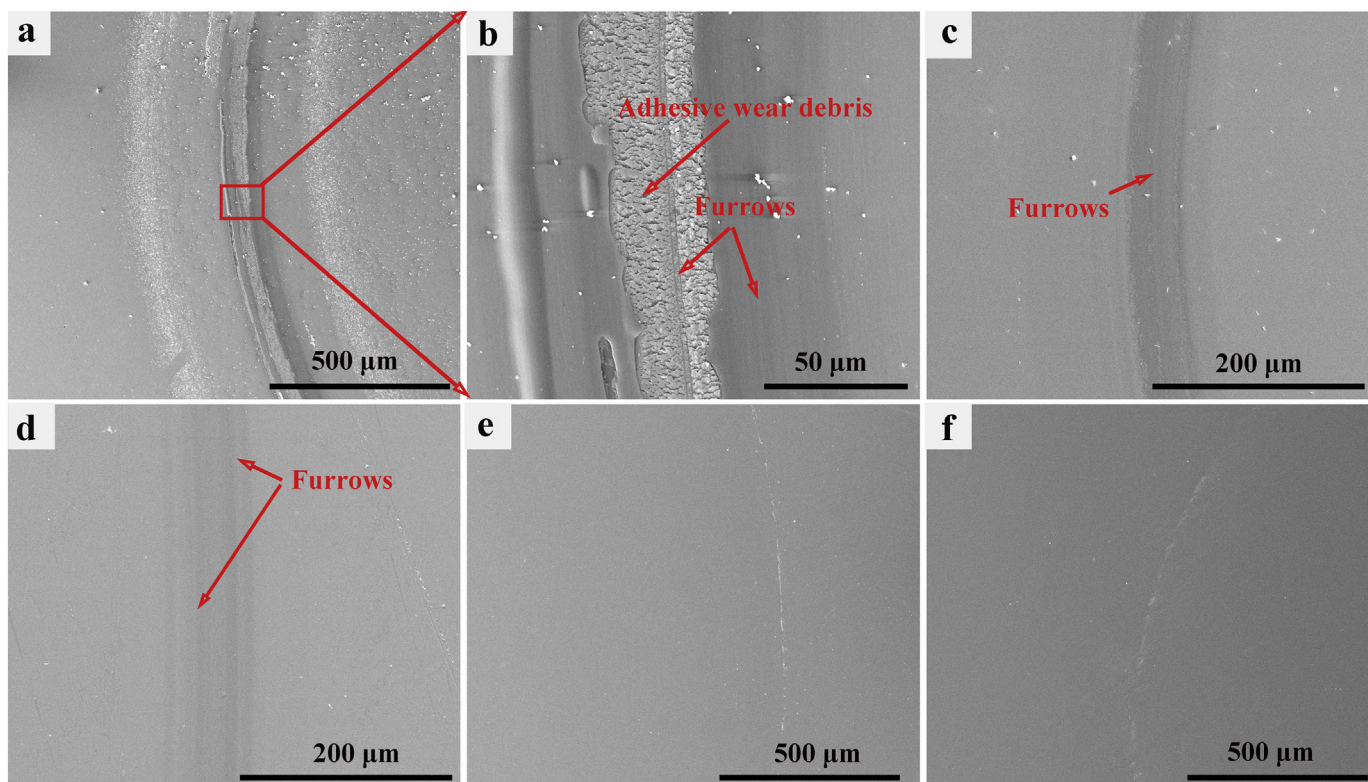


Fig. 9. SEM images of the wear tracks for the Cu/Cr-DLC films deposited at different temperatures: (a) and (b) 60 °C, (c) 100 °C, (d) 150 °C, (e) 200 °C, (f) 250 °C.

distribution maps of wear scars on counterpart steel balls. The elemental distribution analysis of the wear scars included five kinds of elements, which were the Fe, O, Cu, C and Cr, respectively. Each element was marked with a different color, and the density of each color represented the relative content of the corresponding element. It could be identified that the transfer layer was formed on the steel ball counterface for all samples. Besides, wear debris was apparently observed at the deposition temperature below 150 °C. Particularly, there were amount of wear debris accumulated around the wear scars, when the film was deposited at the temperature of 60 °C. The elemental distribution maps showed that the wear debris was composed of much more Cu, O and less carbon. Moreover, the thin transfer layer presented the similar result, implying the formation of a Cu oxide phase. The wear scars corresponding to 100 °C and 150 °C exhibited thick transfer layers, which were presented by Cu, O and a little carbon as well. Subsequently, the wear scars at the temperature of 200 °C and 250 °C were relatively smaller, and no obvious wear debris was observed. The transfer layers displayed a reduced Cu, O and Carbon content. In addition, a continuous and compact transfer film emerged on the steel ball at the deposition temperature of 200 °C, and it mainly contained carbon and a little Cu. However, it was difficult to verify the change of Cr element in the transfer film with different deposition temperatures, because the thickness of the transfer film was sub-micrometer and the Cr in the steel ball could be detected.

In order to obtain further information about the nature of the tribological behavior on the counterface, Raman tests were conducted for the transfer film. Fig. 11 shows the Raman spectra of transfer films on the steel ball after sliding against Cu/Cr-DLC films. As shown in Fig. 11(a), there were several peaks generated at 200  $\text{cm}^{-1}$ , 224  $\text{cm}^{-1}$ , 300  $\text{cm}^{-1}$ , 334  $\text{cm}^{-1}$ , 433  $\text{cm}^{-1}$ , 532  $\text{cm}^{-1}$  and 676  $\text{cm}^{-1}$ , indicating the transfer films formed below 150 °C contained copper oxide phases. According to the related references [30–33], the peaks at 218  $\text{cm}^{-1}$ , 430  $\text{cm}^{-1}$ , 530  $\text{cm}^{-1}$  and 665  $\text{cm}^{-1}$  could be assigned to the characteristic phonon modes of the  $\text{Cu}_2\text{O}$ , while the characteristic peaks of CuO phase were located at 298  $\text{cm}^{-1}$  and 330  $\text{cm}^{-1}$ . Hence one can see

that the peak positions obtained from the transfer film is slightly different from that of the above references. It was demonstrated that the peak deviation or new peak generation was originated from the nanoscale structure of the copper oxide phase. Related reference proved that the size of copper oxide phase could dramatically influence the peak position, peak intensity even the peak numbers of the Raman spectra by the change of the internal vibration mode [34]. In addition, the composition of transfer films depended strongly on the deposition temperature. At 60 °C, the transfer film was mainly composed of  $\text{Cu}_2\text{O}$  phase. With the deposition temperature increased, the composite of transfer film was dominant CuO phase with a little  $\text{Cu}_2\text{O}$  phase. When the deposition temperature reached up to 200 °C and 250 °C, the concentration of Cu metal dramatically decreased, and no copper oxide phase could be observed on the transfer film. However, Cr oxide was absent in the Raman spectra due to the chemical reaction between C and Cr atoms. As shown in Fig. 11(b), the DLC transferred from the film to transfer films was indicated by the presence of D and G peaks at about 1350  $\text{cm}^{-1}$  and 1580  $\text{cm}^{-1}$ , respectively. According to the intensity ratio of D peak to G peak ( $I_D/I_G$ ), increasing the deposition temperature from 60 °C to 200 °C led to the monotonous increase of  $I_D/I_G$  from 0.94 to 3.51, which decreased to 2.63 at 250 °C and was higher than that of the as-deposited film (Fig. 3). Since the graphitization was formed at higher deposition temperatures during the tribological tests, two reasons could be employed to understand this evolution of carbon states. First, Marciano et al. [35] showed clearly that the silver nanoparticles incorporated in the DLC film were beneficial to reduce the reaction of oxygen with carbon. So it is possible for Cu to form copper oxide and reduce the reaction of oxygen with carbon. In such case, the graphitization catalyzing potential of the doped Cu atoms reduced during the sliding process. Second, more copper oxide and Cr–C phase could enhance the thermal stability of the film, which might lead to delay the transforming of some  $\text{sp}^3$  to  $\text{sp}^2$  carbons [36,37].

Based on the observed results, a simple model was proposed to describe the contact between steel ball and Cu/Cr-DLC, as shown in Fig. 12. For DLC film with high Cu/Cr concentration at 60 °C, a strong

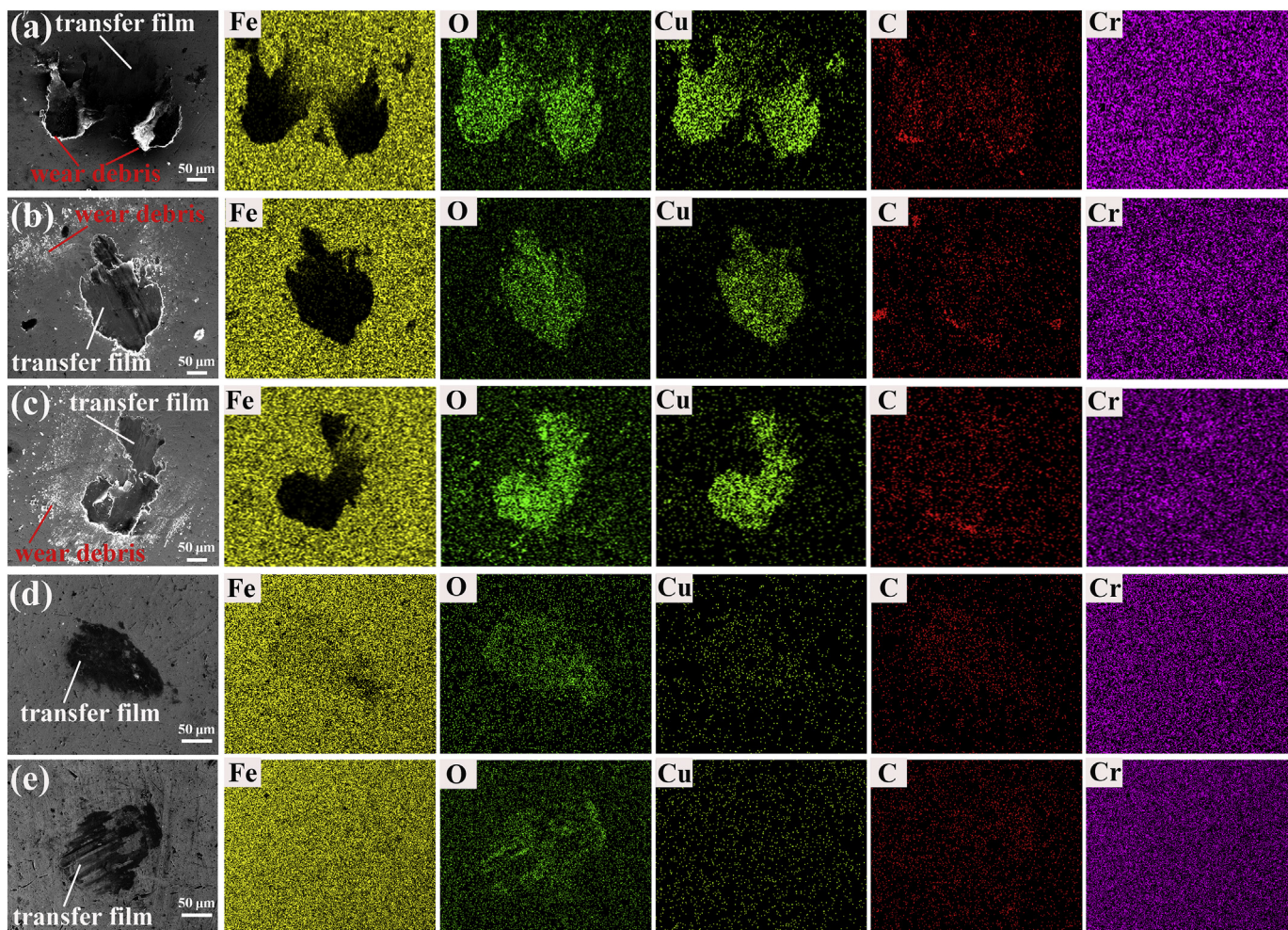


Fig. 10. SEM images and elemental distribution maps of wear scar on steel balls sliding against the Cu/Cr-DLC films deposited at different temperatures: (a) 60 °C; (b) 100 °C; (c) 150 °C; (d) 200 °C; (e) 250 °C.

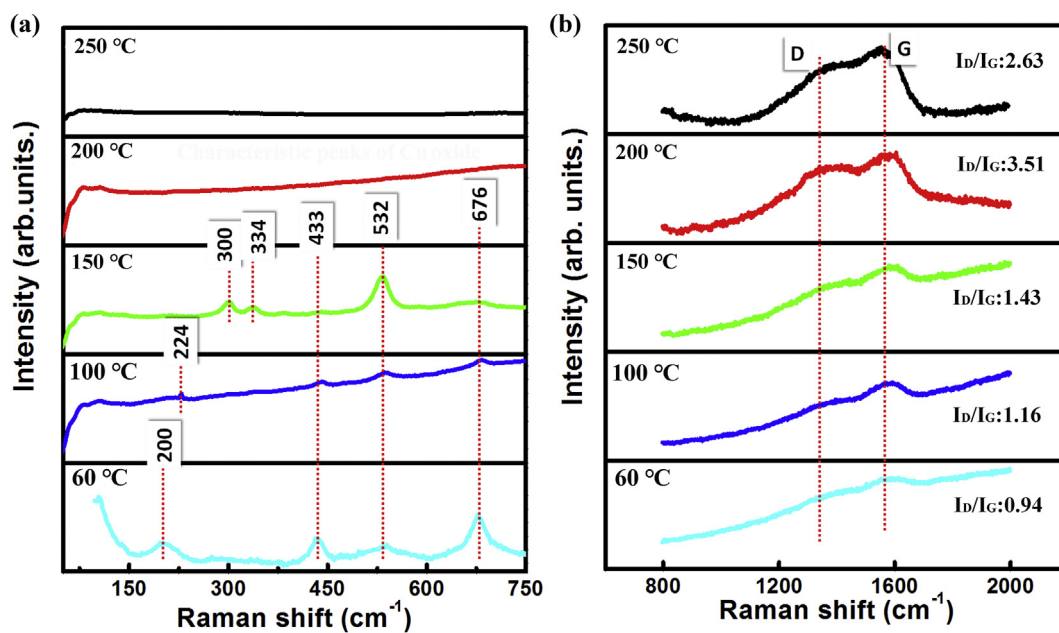


Fig. 11. Raman spectra of transfer films, (a) Raman shift at the range of 0–750 cm<sup>-1</sup>, (b) Raman shift at the range of 800–2000 cm<sup>-1</sup>.

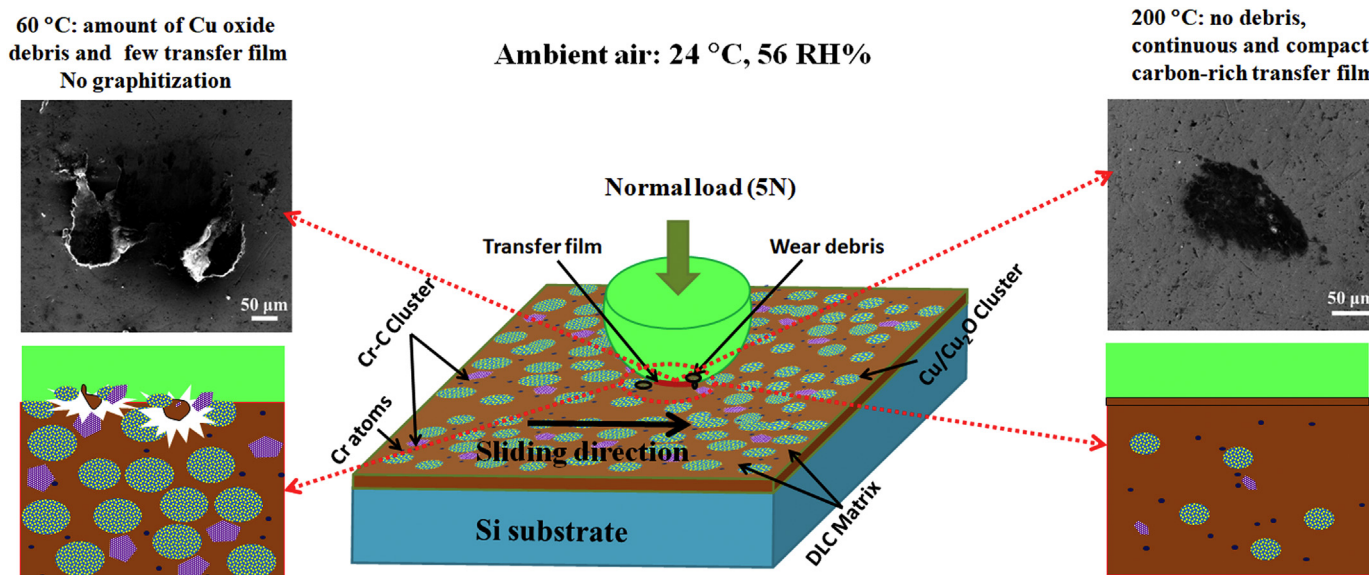


Fig. 12. Schematic description of wear mechanism for Cu/Cr-DLC films deposited at different temperatures.

adhesive bond is occurred between the contacting asperities, leading to severe plastic shearing at the junction [38–40]. Fig. 11 showed the confirmation that the presence of tribolayer generated a dynamic adhesion with primarily oxidative wear. Moreover, the XPS (Fig. 4) results indicated that an obvious abrasive wear was caused by the formed hard Cr–C phase in the film. In this case, the friction coefficient remained high due to shearing and extrusion of the soft Cu material in and out of the contact [25]. Hence, the film was seriously worn out. Representatively, for Cu/Cr-DLC film at the deposition temperature of 200 °C, A continuous and compact transfer film forming on the counterface prevented the direct contact between two surfaces. In addition, graphitization induced on the sliding interface in the friction process, was assumed to play an important role in decreasing the friction coefficient and wear volume [37]. Moreover, the H/E ratio is a suitable parameter for predicting wear resistance [41], the higher the H/E ratio, the higher the resistance to wear of films. The H/E ratio of the films deposited at 200 °C was higher than that of films at low deposition temperatures, showing better wear resistances at the same friction condition. It was illustrated that good mechanical properties and the continuous graphitized transfer film were the main reasons for excellent tribological performances of Cu/Cr-DLC films deposited at high temperature.

#### 4. Conclusions

In the present work, Cu/Cr-DLC films were deposited via a hybrid system combined with a DC magnetron sputtering source and a linear ion source. The mechanical and tribological properties were discussed in terms of the evolution of chemical composition and microstructure at different deposition temperature. Results revealed that the elemental compositions of Cu/Cr-DLC films were tailored by the deposition temperature. As the deposition temperature rose, the concentrations of Cu and Cr decreased, and the formation of Cr carbide was promoted, which resulted in the improvement of the hardness and toughness of the Cu/Cr-DLC films. Although the residual stress of the film deposited at 200 °C was higher than that of films deposited below 150 °C, It presented excellent adhesion and friction performance. The superior mechanical properties and the formation of graphitization transfer film were the main reasons for the good wear resistance behavior at high deposition temperature.

#### Acknowledgments

The work was supported by the National Natural Science Foundation of China (51601211), Ningbo Science and Technology Innovation Project (2018B10014), Major Science and Technology Project of Jiangbei District, Ningbo (201801A03) and Special Research and Development Project of Jiangxi Province (2018-YZD2-15).

#### References

- [1] H. Dimigen, H. Hübsch, Applying low-friction wear-resistant thin solid films by physical vapor deposition, *Philips Tech. Rev.* 41 (1983–1984) 186–197.
- [2] H. Dimigen, H. Hübsch, R. Memming, *Appl. Phys. Lett.* 50 (1987) 1056–1058.
- [3] K. Bewilogua, D. Hofmann, History of diamond-like carbon films – from first experiments to worldwide applications, *Surf. Coat. Technol.* 242 (2014) 214–225.
- [4] H.S. Hsu, P.E. Lu, C.W. Chang, S.J. Sun, C.H. Lee, H.C. Su, Y.Y. Chin, H.J. Lin, C.T. Chen, M.J. Huang, Tunable interfacial magnetic-optical properties of Co doped amorphous carbon film induced by charge transfer after acid treatment, *Carbon* 77 (2014) 398–404.
- [5] L. Ji, H.X. Li, F. Zhao, W.L. Quan, J.M. Chen, H.D. Zhou, Atomic oxygen resistant behaviors of Mo/diamond-like carbon nanocomposite lubricating films, *Appl. Surf. Sci.* 255 (2009) 4180–4184.
- [6] J.X. Huang, L.P. Wang, B. Liu, S.H. Wan, Q.J. Xue, In vitro evaluation of the tribological response of Mo-doped graphite-like carbon film in different biological media, *ACS Appl. Mater. Interfaces* 7 (2015) 2772–2783.
- [7] F. Zhao, H.X. Li, L. Ji, Y.J. Wang, H.D. Zhou, J.M. Chen, Ti-DLC films with superior friction performance, *Diam. Relat. Mater.* 19 (2010) 342–349.
- [8] A. Amanov, T. Watabe, R. Tsuboi, S. Sasaki, Fretting wear and fracture behaviors of Cr-doped and non-doped DLC films deposited on Ti–6Al–4V alloy by unbalanced magnetron sputtering, *Tribol. Int.* 62 (2013) 49–57.
- [9] A.Y. Wang, K.R. Lee, J.P. Ahn, J.H. Han, Structure and mechanical properties of W incorporated diamond-like carbon films prepared by a hybrid ion beam deposition technique, *Carbon* 44 (2006) 1826–1832.
- [10] X. Yu, Y. Qin, C.B. Wang, Y.Q. Yang, X.C. Ma, Effects of nanocrystalline silver incorporation on sliding tribological properties of Ag-containing diamond-like carbon films in multi-ion beam assisted deposition, *Vacuum* 89 (2013) 82–85.
- [11] M.Y. Tsai, M.S. Huang, L.K. Chen, Y.D. Shen, M.H. Lin, Y.C. Chiang, K.L. Ou, S.F. Ou, Surface properties of copper-incorporated diamond-like carbon films deposited by hybrid magnetron sputtering, *Ceram. Int.* 39 (2013) 8335–8340.
- [12] G.A. Zhang, P.X. Yan, P. Wang, Y.M. Chen, J.Y. Zhang, The preparation and mechanical properties of Al-containing a-C: H thin films, *J. Phys. D: Appl. Phys.* 40 (2007) 6748–6753.
- [13] Q. Li, K.X. Gao, L.F. Zhang, J. Wang, B. Zhang, J.Y. Zhang, Further improving the mechanical and tribological properties of low content Ti-doped DLC film by W incorporating, *Appl. Surf. Sci.* 353 (2015) 522–529.
- [14] S.G. Zhou, L.P. Wang, S.C. Wang, Q.J. Xue, Comparative study of simplex doped nc-WC/a-C and duplex doped nc-WC/a-C(AI) nanocomposite coatings, *Appl. Surf. Sci.* 257 (2011) 6971–6979.
- [15] X.W. Li, L.L. Sun, P. Guo, P.L. Ke, A.Y. Wang, Structure and residual stress evolution of Ti/Al, Cr/Al or W/Al co-doped amorphous carbon nanocomposite films: insights from ab initio calculations, *Mater. Des.* 89 (2016) 1123–1129.
- [16] X.W. Li, P. Guo, L.L. Sun, A.Y. Wang, P.L. Ke, Ab initio investigation on the novel

- Cu/Cr co-doped amorphous carbon nanocomposite films with giant residual stress reduction, *ACS Appl. Mater. Interfaces* 7 (2015) 27878–27884.
- [17] L. Ji, Y.X. Wu, H.X. Li, H. Song, X.H. Liu, Y.P. Ye, J.M. Chen, H.D. Zhou, L. Liu, The role of trace Ti concentration on the evolution of microstructure and properties of duplex doped Ti (Ag)/DLC films, *Vacuum* 115 (2015) 23–30.
- [18] S.E. Ong, S. Zhang, H.J. Du, G. Tan, Temperature effect on bonding structures of amorphous carbon containing more than 30at.% silicon, *Diam. Relat. Mater.* 16 (2007) 1823–1827.
- [19] A.M. Asl, P. Kameli, M. Ranjbar, H. Salamati, M. Jannesari, Correlations between microstructure and hydrophobicity properties of pulsed laser deposited diamond-like carbon films, *Superlattice. Microst.* 81 (2015) 64–79.
- [20] L.L. Sun, P. Guo, X.W. Li, A.Y. Wang, Synergistic effect of Cu/Cr co-doping on the wettability and mechanical properties of diamond-like carbon films, *Diam. Relat. Mater.* 68 (2016) 1–9.
- [21] W. Dai, H. Zheng, G.S. Wu, A.Y. Wang, Effect of bias voltage on growth property of Cr-DLC film prepared by linear ion beam deposition technique, *Vacuum* 85 (2010) 231–235.
- [22] D. Depla, On the effective sputter yield during magnetron sputter deposition, *Nucl. Inst. Methods Phys. Res. B* 328 (2014) 65–69.
- [23] X.Q. Liu, J.Y. Hao, Y.T. Xie, Silicon and aluminum doping effects on the microstructure and properties of polymeric amorphous carbon films, *Appl. Surf. Sci.* 379 (2016) 358–366.
- [24] C. Casiraghi, A.C. Ferrari, R. Ohr, D. Chu, J. Robertson, Surface properties of ultrathin tetrahedral amorphous carbon films for magnetic storage technology, *Diam. Relat. Mater.* 13 (2004) 1416–1421.
- [25] C. Donnet, A. Erdemir, *Tribology of Diamond-like Carbon Film*, Springer, Boston, 2008, pp. 311–338.
- [26] B. Bhushan, Nanotribology of ultrathin and hard amorphous carbon films, in: B. Bhushan (Ed.), *Springer Handbook of Nanotechnology*, Springer, Berlin Heidelberg, 2004, pp. 791–830.
- [27] W. Dai, A.Y. Wang, Q.M. Wang, Microstructure and mechanical property of diamond-like carbon films with ductile copper incorporation, *Surf. Coat. Technol.* 272 (2015) 33–38.
- [28] J.J. Jiang, H. Huang, Q. Wang, S.M. Wang, Z.Q. Wei, H. Yang, J.Y. Hao, Effect of the deposition temperature on growth, structure and mechanical properties of diamond-like carbon films co-doped by titanium and silicon, *Acta Phys. Sin.* 63 (2014) 028104.
- [29] J. Musil, Hard nanocomposite coatings: thermal stability, oxidation resistance and toughness, *Surf. Coat. Technol.* 207 (2012) 50–65.
- [30] J. Li, Y.H. Liu, T.Q. Wang, X.C. Lu, Chemical effects on the tribological behavior during copper chemical mechanical planarization, *Mater. Chem. Phys.* 153 (2015) 48–53.
- [31] H. Solache-Carranco, G. Juárez-Díaz, J. Martínez-Juárez, Y.R. Peña-Sierra, Estudio de la cristalización de Cu<sub>2</sub>O y su caracterización por difracción de rayos X, espectroscópica Raman y fotoluminiscencia, *Rev. Mex. Fis.* 55 (2009) 393–398 (in Spanish).
- [32] Y.C. Mao, J.T. He, X.F. Sun, W. Li, X.H. Lu, J.Y. Gan, Z.Q. Liu, L. Gong, J. Chen, P. Liu, Y.X. Tong, Electrochemical synthesis of hierarchical Cu<sub>2</sub>O stars with enhanced photoelectrochemical properties, *Electrochim. Acta* 62 (2012) 1–7.
- [33] R.L. Papurello, Ana P. Cabello, M.A. Ulla, C.A. Neyertz, J.M. Zamaro, Microreactor with copper oxide nanostructured films for catalytic gas phase oxidations, *Surf. Coat. Technol.* 328 (2017) 231–239.
- [34] D. Sun, P.G. Yin, L. Guo, Synthesis and Raman property of porous jujube-like Cu<sub>2</sub>O hierarchy structure, *Acta Phys. -Chim. Sin.* 27 (2011) 1543–1550.
- [35] F.R. Marciano, L.F. Bonetti, R.S. Pessoa, J.S. Marcuzzo, M. Massi, L.V. Santos, V.J. Trava-Airoldi, The improvement of DLC film lifetime using silver nanoparticles for use on space devices, *Diam. Relat. Mater.* 17 (2008) 1674–1679.
- [36] N. Salah, A. Alshahrie, J. Iqbal, P.M.Z. Hasan, M.Sh. Abdel-wahab, Tribological behavior of diamond-like carbon thin films deposited by the pulse laser technique at different substrate temperatures, *Tribol. Int.* 103 (2016) 274–280.
- [37] I.C. Müller, J. Sharp, W.M. Rainforth, P. Hovsepian, A. Ehasarian, Tribological response and characterization of Mo-W doped DLC coating, *Wear* 376–377 (2017) 1622–1629.
- [38] A.T.M.A. Rahman, A.C. Frangeskou, M.S. Kim, S. Bose, G.W. Morley, P.F. Barker, Buring and graphitization of optically levitated nanodiamonds in vacuum, *Sci. Rep.* 6 (2016) 21633.
- [39] J.A. Greenwood, D. Tabor, Deformation properties of friction junctions, *Proc. Phys. Soc. B* 68 (1955) 609–619.
- [40] C.A. Brockley, G.K. Fleming, A model junction study of severe metallic wear, *Wear* 8 (1965) 374–380.
- [41] A. Leyland, A. Matthews, On the significance of the H/E ratio in wear control: a nanocomposite coating approach to optimized tribological behaviour, *Wear* 246 (2000) 1–11.